Deformation and Suction Variation of an Unsaturated Soil during Constant Water Content Triaxial Loading

L. Li
Department of Civil Engineering, University of Alaska Anchorage, Anchorage, AK, USA

X. Zhang
Civil, Architectural and Environmental Engineering, Missouri University of Science and Technology, Rolla, MO, USA

ABSTRACT: Triaxial tests are widely used to characterize the stress strain behaviour of unsaturated soils. Previous studies indicated that the soil stress strain characteristics were highly dependent on the shear plane evolution process during testing. In this study, a newly developed triaxial testing system was adopted to characterize the behaviour of an unsaturated soil. In this triaxial system, the soil deformation and suction were measured using a photogrammetry-based method and high-capacity tensiometers, respectively. To investigate the behaviour of unsaturated soils, a series of triaxial tests were conducted on soils with different moisture contents under different confining stress levels. Based on the soil suction and deformation measurement results, the soil suction variation and shear plane evolution process were characterized for soils sheared under different confining stresses.

1 INTRODUCTION

Triaxial tests are commonly used to characterize both saturated and unsaturated soils. During testing, the soil volume change is required to be measured for soil behaviour characterization. However, according to recent findings (e.g. Alshibli et al. 2000; Rechenmacher and Saab 2002; Desrues 2004; and Rechenmacher 2006), soil stress strain characteristics were also highly dependent on the shear plane evolution during testing. In Sachan and Penumadu (2007), the localized strain was considered to be a major factor which controls the overall mechanical response of the soil, at or near failure. As a result, an accurate experimental quantification of shear band formation, growth, and evolution is very critical for characterizing unsaturated soil behaviour under triaxial loading conditions. Due to this reason, more and more attention was drawn on the investigation of localized deformation in soil during triaxial testing. (Lin and Penumadu 2006; Rechenmacher 2006; Sachan and Penumadu 2007; Rechenmacher and Medina-Cetina 2007; and Bhandari et al. 2012).

In Lin and Penumadu (2006) and Sachan and Penumadu (2007), strain localization during testing was measured based on tracking the deformation of a point grid on soil surface using a digital camera. However, there are several limitations such as sophisticated distortion calibration and poor measurement accuracy associated with this method. Besides the digital image analysis method, the digital image correlation technique was also reported to be utilized for soil deformation measurements under triaxial conditions (e.g. Rechenmacher 2006; Rechenmacher and Medina-Cetina 2007; and Bhandari et al. 2012). In this method, the deformation measurement was derived by mapping, between digital images, overlapping subsets of pixels or overlapping clusters of sand grains at many points across the specimen surface. Detailed soil deformation could be extracted using this method. However, in Rechenmacher (2006) and Rechenmacher and Medina-Cetina (2007), due to the difficulties in dealing with refraction, this method cannot be directly used for deformation measurements on soils located in a triaxial chamber. Bhandari et al. (2012) reported the use of digital image correlation technique for soil deformation measurements under triaxial conditions. A three-dimensional (3D) refraction model was derived to correct the refractions at the interfaces of air-cell and cell-water. Three cameras around the triaxial testing system at an interval of 120° were used to capture images of the soil at different loading steps. However, this deformation measurement method suffered several limitations as summarized in Li et al. (2015).

In this study, a new unsaturated soil triaxial testing system was applied to measure the full field 3D deformation of an unsaturated soil during testing. With this system, the suction variation and full field deformation process of the unsaturated soil was successfully recorded in very high accuracy. The results from this triaxial test can be used for more advanced unsaturated soil behaviour characterization.

2 MATERIALS AND TRIAXIAL TESTS

2.1 *Test setup*

The new triaxial testing system, developed by Li and Zhang (2015) based on a conventional triaxial test apparatus for saturated soils, as shown in Figure 1a, was adopted for the constant water content triaxial test during which the pore-air was vented to atmosphere. In this system, to facilitate the deformation measurement, some measurement targets are posted to the acrylic cell and the membrane (with soil specimen inside). A non-contact photogrammetry-based method developed by Zhang et al. (2015) and Li et al. (2016) was used to accurately measure the 3D models of unsaturated soils during triaxial testing. In this system, besides this volume measurement, instead of controlling suction, new miniature high-capacity tensiometers, as shown in Figure 1b, are utilized to monitor matric suction variations during the constant water content triaxial tests. This type of tensiometer was developed by replacing the porous stone of an EPB-PW miniature pressure transducer (http://www.te.com) with a 15 bar air-entry value ceramic disc as shown in Figure 1c. With two of these high-capacity tensiometers, direct soil suction measurements were made at the middle of the soil specimen as shown in Figure 1a which eliminated the influence of the end effect.

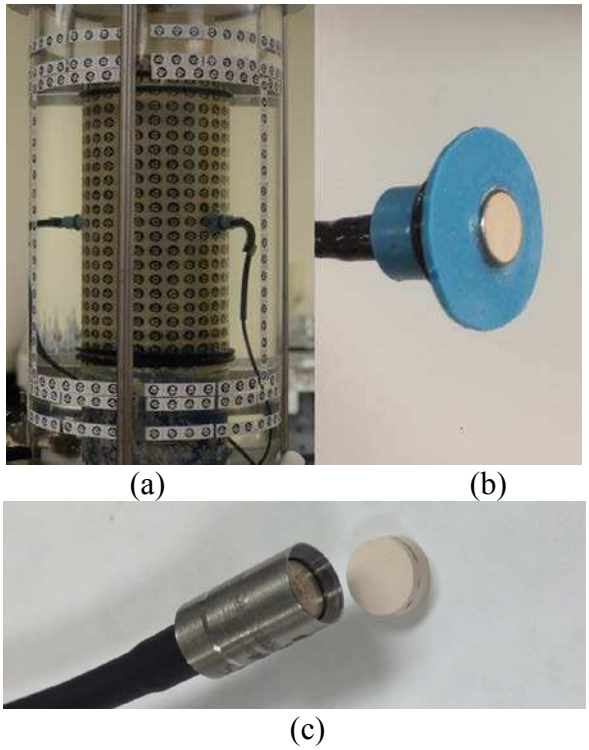

(a) (b)

(c)

Figure 1. Triaxial testing system and high-capacity tensiometer.

2.2 *Soil type and index properties*

Silt mixed with Kaolin at a ratio of 85:15 was used to fabricate the unsaturated soil specimens for the triaxial tests. The optimal moisture content and maximum dry density are 15% and 1.836 g/cm^3, respectively. The plastic and liquid limits of the soil are 18.2% and 19.7%, respectively. The specific gravity of the soil is 2.7. After that, the soil was compacted in 10 layers to 71 mm in diameter and 142 mm in height soil cylinders at a water content of 16% using the under-compaction procedure (Ladd 1978). The soil specimens were then conditioned to different moisture contents by controlling the number of exposures to atmosphere for about 15 minutes/day. Finally, the soil specimens were sealed in plastic bags and stored in a moisture room for at least one month to ensure suction equilibrium in the whole soil specimen. In this study, three unsaturated specimens at moisture contents of 11.36%, 12.23%, and 12.14% were tested under different net confining pressure levels of 10 kPa, 50 kPa, and 100 kPa, respectively. In this study, step load was applied to the specimens during testing since the soil suction required a certain time to reach equilibrium after a loading process. During testing, the inside of the soil specimen was vented to the atmosphere to ensure a pore-air pressure of 0 kPa throughout the test.

3 TEST RESULTS

After three triaxial tests, with the photogrammetry-based method, the soil volume changes and stress-strain behaviour during loading were obtained and plotted in Figure 2. The recorded peak load of three specimens increased with increasing confining pressure. Failure planes were observed during loading for the soil specimens sheared under net confining pressures of 10 kPa and 50 kPa as shown in Figure 3. The soil specimen sheared under a net confining pressure of 100 kPa gradually turned into barrel-shaped during triaxial loading. The specimens sheared under net confining pressures of 50 kPa and 100 kPa experienced a volume decrease and then a shear dilation process during loading as shown in Figure 2b. For the soil specimen sheared under a net confining pressure of 10 kPa, the soil volume continuously increased during testing due to the applied low confining stress.

Besides volume change, the soil suction variation during testing was recorded by two high-capacity tensiometers, as shown in Figure 4, during loading. The suction of the soil specimen sheared under 10 kPa net confining pressure was the highest due to its lowest moisture content. Generally, during triaxial loading, the soil suction decreased. After each loading step, the soil suction quickly decreased and the gradually reached a new equilibrium. This was due to that a certain time was required for the dissipation of the pore water and air pressure after a loading process. The soil suction variation recorded by two tensiometers were in agreement before reaching the failure point and slightly varied after the failure point especially for the soils sheared under net confining pressures of 10 kPa and 50 kPa.

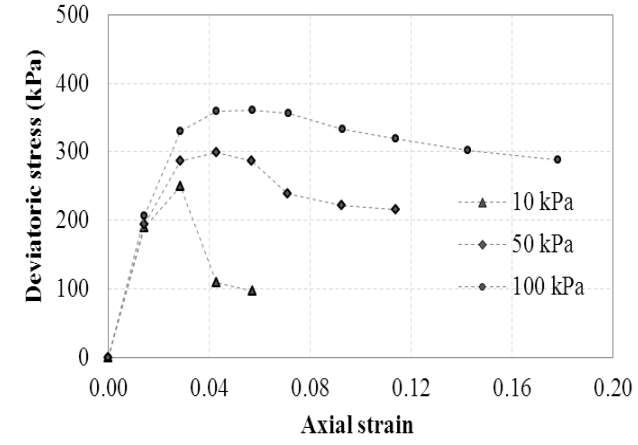

(a)

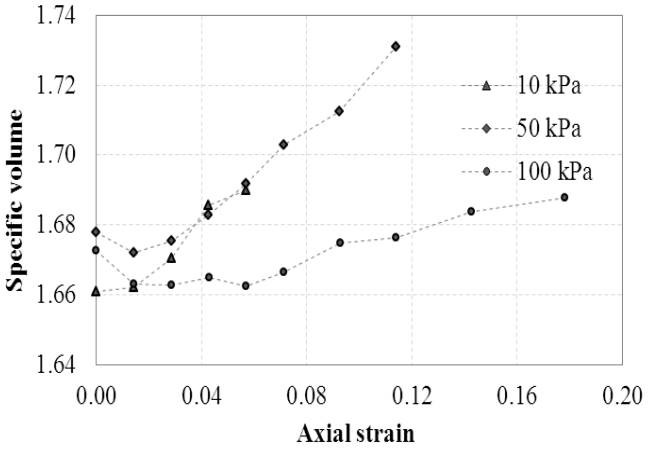

(b)

Figure 2. Results for triaxial tests conducted at different confining stresses (10, 50, and 100 kPa).

Figure 3. Soil specimens after the triaxial test.

This was reasonable since the presence of the shear plane broke the soil specimen into two parts and the volumetric strain in two parts might not be uniform. Consequently, the soil suction in the two sections was different due to the difference in their volumetric strains.

With the 3D coordinates of the targets on soil surface at different loading steps during testing, the deformation of three specimens could then be extracted. By connecting each point with the adjacent points, triangular meshes were generated which demonstrated the soil shapes at different loading levels.

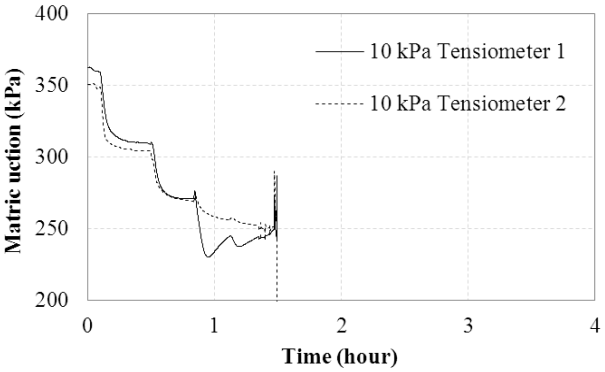

(a)

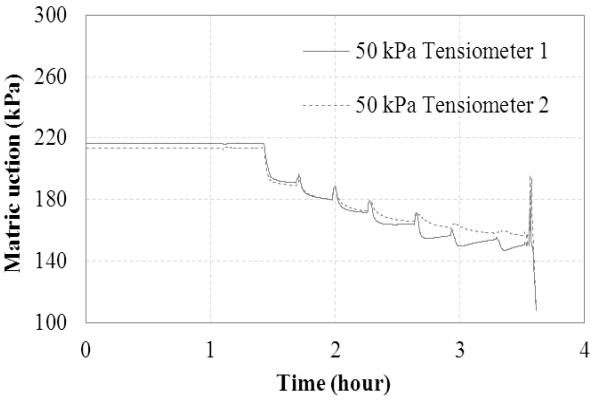

(b)

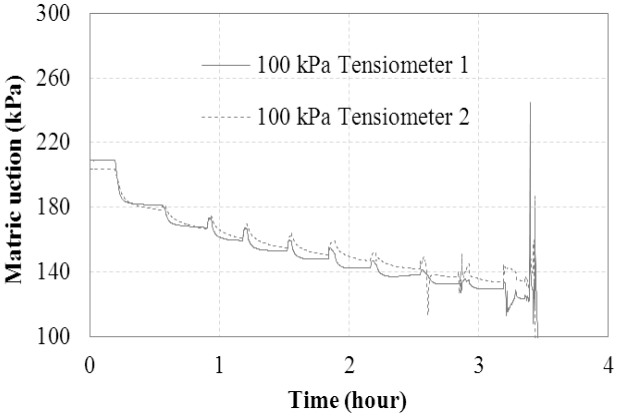

(c)

Figure 4. Suction variation during triaxial loading.

Figure 5 shows the deformations of three specimens during shearing under 10 kPa, 50 kPa, and 100 kPa net confining pressures and different axial displacements, respectively. When shearing under a net confining pressure of 10 kPa, the specimen remained approximately cylindrical throughout the test. With an increase in the axial displacement, a shear band gradually formed in the soil specimen and finally the soil specimen failed due to the applied deviatoric load. Similar results were also found on the specimen sheared under a net confining pressure of 50 kPa. However, for the specimen sheared under a net confining pressure of 100 kPa, with an increase in the axial displacement, the soil specimen gradually deformed into a barrel-shape as shown in Figure 3. The diameter of the specimen at the middle was the largest and narrows towards the two ends.

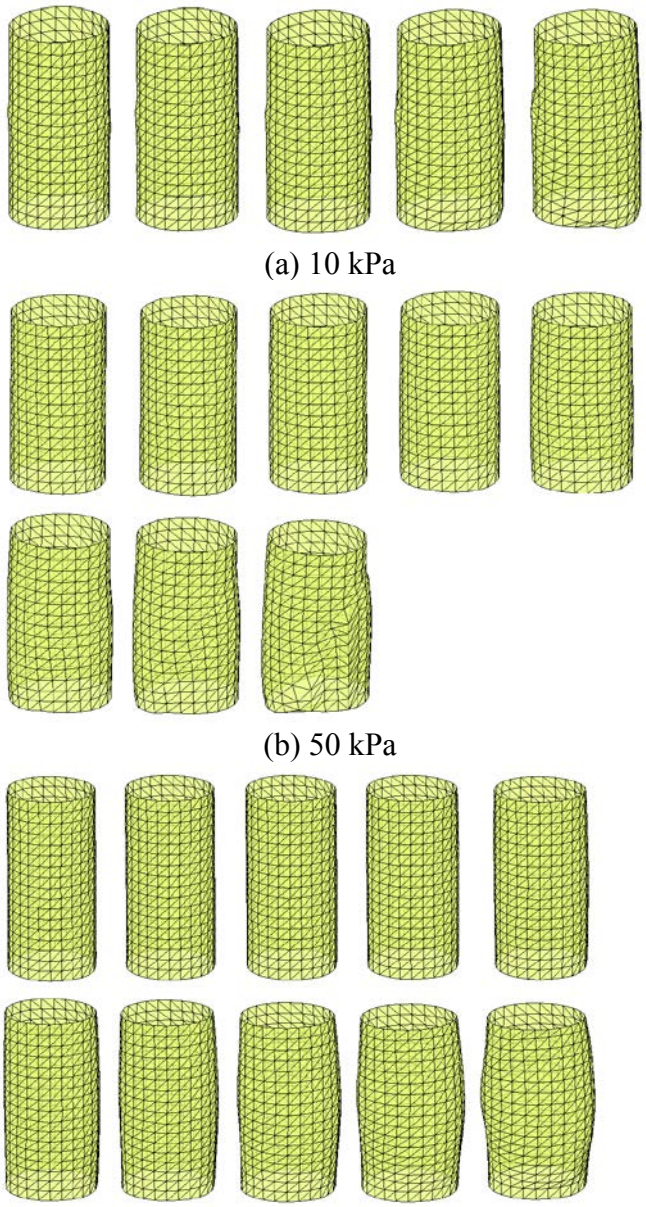

(a) 10 kPa

(b) 50 kPa

(c) 100 kPa

Figure 5. Soil deformation triaxial loading.

The shapes were reasonable since the friction between the soil and the loading platens restrained soil from deforming at both ends. The results were reasonable and consistent with previous studies (Li and Zhang 2015).

With the 3D coordinates of the targets on soil surface at different loading steps during testing, the full field axial strain distribution of three specimens was then extracted as shown in Figure 6. A clear shear plane was shown on for specimens sheared under net confining pressures of 10 kPa and 50 kPa. For the specimen shear under a net confining pressure of 10 kPa, as shown in Figure 6a, the specimen broke into two parts and the top part was sliding over the lower part which was consistent with the observation on Figure 3 after testing. The localized strain occurred at the failure plane at a displacement level of 6 mm. The strain in the lower and upper part of the soil was at a very low level when compared with the strain at the failure plane.

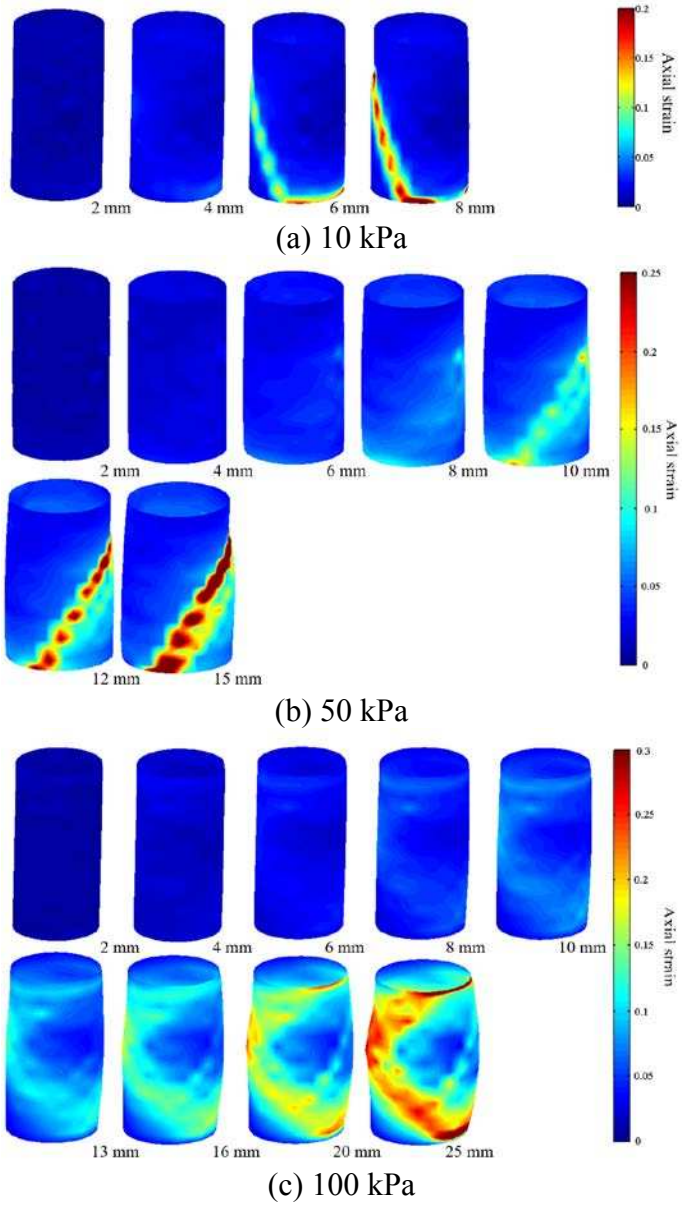

(a) 10 kPa

(b) 50 kPa

(c) 100 kPa

Figure 6. Axial strain distribution during triaxial loading.

For the specimen shear under a net confining pressure of 50 kPa, as shown in Figure 6b, the failure plane occurred at a displacement level of 10 mm due to the increased confining stress. Different from the specimens sheared under net confining pressures of 10 kPa and 50 kPa, no clear shear band was observed on the specimen as shown in Figure 3. The observation is consistent with the axial strain results as shown in Figure 6c. However, a "V" shape localized strain can still be found. The reason for the distorted strain contours was attributed to the triaxial load applied to the soil was eccentric and the non-uniformity of the specimen.

4 CONCLUSIONS

A new triaxial testing system is adopted to investigate the behaviour of an unsaturated during triaxial testing. In this system, the soil suction and deformation were measured using two high-capacity tensiometers and a photogrammetry-based method, re-

spectively. Through a series of constant water content triaxial tests on three unsaturated soils, the soil suction and deformation behaviour were investigated. The soil suction variation recorded by two tensiometers during loading were in agreement, which indicated uniform soil suction in the soil, before the presence of a failure plane in the soil. Soil suction non-uniformity was identified after the failure point. Based upon the deformation measurement result, soil deformation was found to be not uniformly distributed throughout the triaxial loading process. During loading, a clear shear band evolution process was captured based upon the axial strain analysis results of soils sheared at 10 kPa and 50 kPa net confining stresses. However, the soil specimen sheared under a confining stress of 100 kPa gradually turned into barrel-shaped during loading due to the end effect.

5 REFERENCES

Alshibli, K.A., Sture, S., Costes, N.C., Frank, M.L., Lankton, M.R., Batiste, S.N. & Swanson, R.A. 2000. Assessment of local deformation in sand using X-ray computed tomography. *Geotechnical Testing Journal*, ASTM 23(3): 274-299.

Bhandari, A.R., Powrie, W. & Harkness, R.M. 2012. A digital image-based deformation measurement system for triaxial tests. *Geotechnical Testing Journal*, ASTM 35(2): 209-226.

Desrues, J. 2004. Tracking strain localization in geomaterials using computerized tomography. *X-ray CT for Geomaterials*: 15-41.

EPB-PW miniature pressure transducer: http://www.te.com/usa-en/product-CAT-PTT0004.html?q=&n=140386&type=products&samples=N

Ladd, R.S. 1978. Preparing Test Specimens Using Under compaction. *Geotechnical Testing Journal*, ASTM 1(1): 16-23.

Li, L. & Zhang, X. 2015. A New Triaxial Testing System for Unsaturated Soil Characterization. *Geotechnical Testing Journal*, ASTM 38(6): 823-839.

Li, L., Zhang, X., Chen, G. & Lytton, R. 2016. Measuring Unsaturated Soils Deformations during Triaxial Testing using a Photogrammetry-Based Method. *Canadian Geotechnical Journal* 53(3): 472-489.

Lin, H. & Penumadu, D. 2006. Strain localization in combined axial-torsional testing on kaolin clay, *Journal of Engineering Mechanics* 132(5): 555-564.

Rechenmacher, A.L. 2006. Grain-scale processes governing shear band initiation and evolution in sands. *Journal of the Mechanics and Physics of Solids* 54(1): 22-45.

Rechenmacher, A.L. & Medina-Cetina, Z. 2007. Calibration of soil constitutive models with spatially varying parameters. *Journal of Geotechnical and Geoenvironmental Engineering*, ASCE 133(12): 1567-1576.

Rechenmacher, A. & Saab, N. 2002. Digital image correlation (DIC) to evaluate progression and uniformity of shear bands in dilative sands. *Proceedings of the 15th ASCE Engineering Mechanics Conference*, Columbia University, NY. June 5.

Sachan, A. & Penumadu, D. 2007. Strain localization in solid cylindrical clay specimens using digital image analysis technique. *Soils and Foundations* 47(1): 67-78.

Zhang, X., Li, L., Chen, G. & Lytton, R. 2015. A Photogrammetry-based Method to Measure Volume Changes of Unsaturated Soil Specimens during Triaxial Testing. *Acta Geotechnica* 10(1): 55-82.